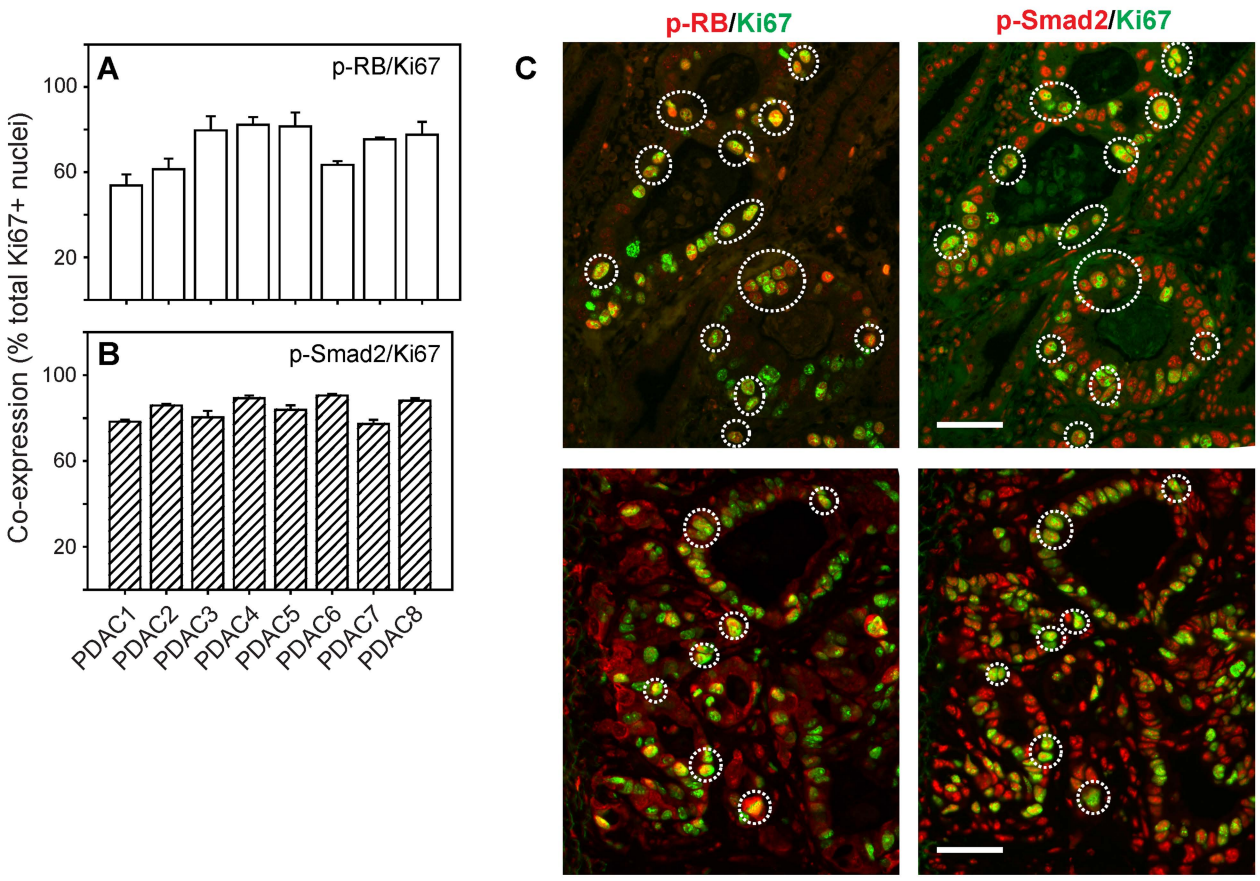

Supplemental Figure 1. RB and Smad2 are frequently phosphorylated in proliferating PDAC cells. **(A-B)** Quantitation of eight human PDACs (PDAC1-8) shows that the average percentage of Ki67-positive PCCs that co-express phospho-RB (A) or phospho-Smad2 (B) is 72% or 84%, respectively. Data are presented as the mean percent ± SEM of Ki67-positive (Ki67+) PCCs that co-express phospho-RB (p-RB/Ki67) or phospho-Smad2 (p-Smad2/Ki67). **(C)** Double immunofluorescence for p-RB (red, left panels) and Ki67 (green), or p-Smad2 (red, right panels) and Ki67 using 3 μm serial sections shows that p-RB, p-Smad2 and Ki67 are abundant in PCC nuclei and frequently overlap (dashed circles). Shown are representative images from two PDACs. Scale Bars, 50 μm.

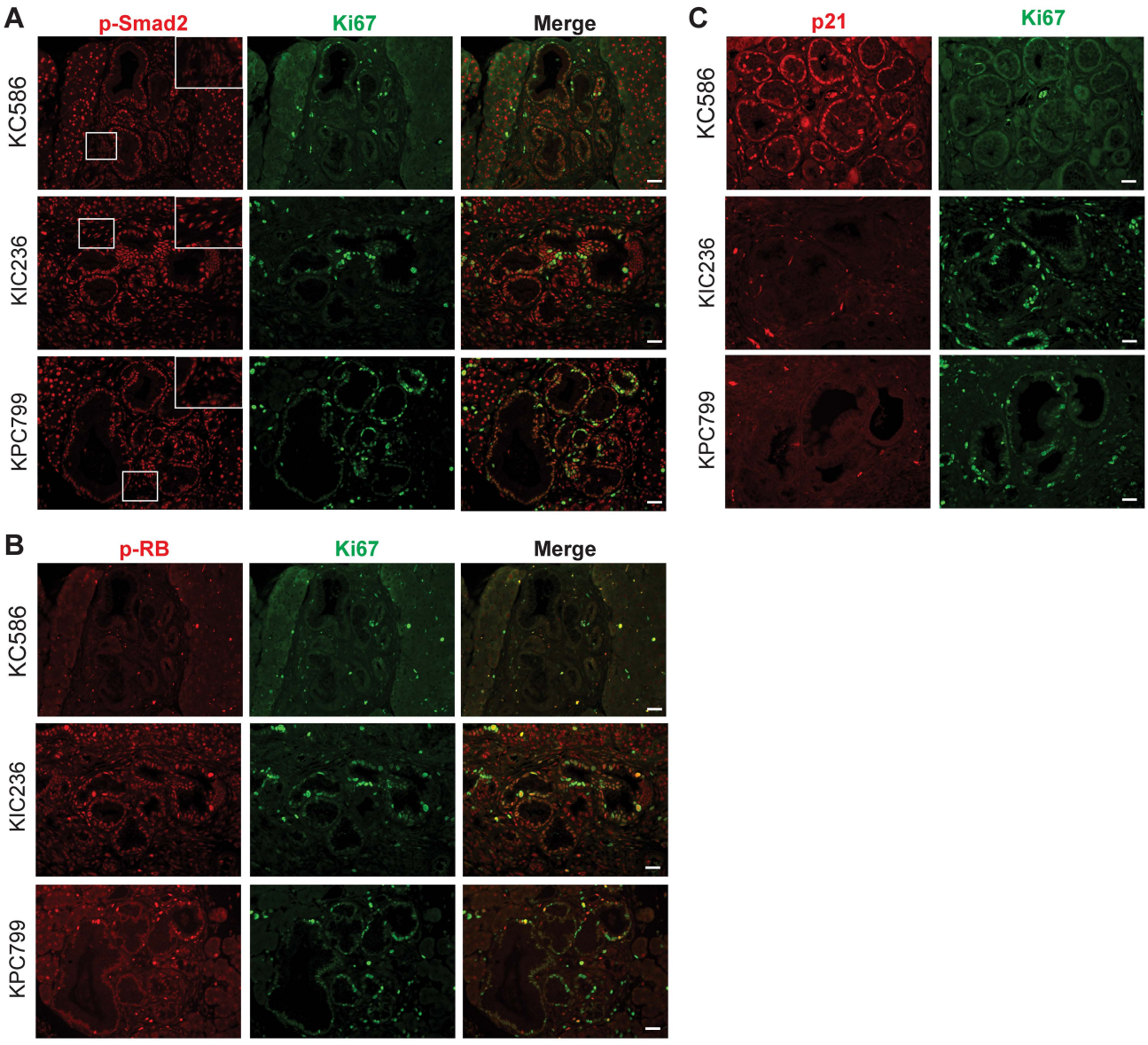

Supplemental Figure 2. RB is inactive in proliferating KIC and KPC PanIN with active Smad2. **(A)** Nuclear p-Smad2 (red) is present in KC, KIC and KPC PanIN and adjacent stromal cells (insets; magnified images of boxed areas). In KC PanIN, Ki67 (green) is rarely detected, whereas KIC and KPC PanIN exhibit Ki67-positive nuclei that harbor p-Smad2 as evidenced by the overlay (merge,). **(B)** In KC PanIN, p-RB (red) is absent and Ki67 is rare, whereas in KIC and KPC PanIN, nuclear p-RB is present and frequently overlaps with Ki67 as evidenced by the overlay (merge). **(C)** $p21^{Waf1}$ (red) is abundant in KC PanIN that lack Ki67 (green, serial sections), but absent in KIC and KPC PanIN that contain Ki67-positive nuclei. Shown are representative images from one of four different 8 month old KC (KC586), or 2 month old KIC (KIC236) and KPC (KPC799) pancreata. Scale Bars, 50 μm.

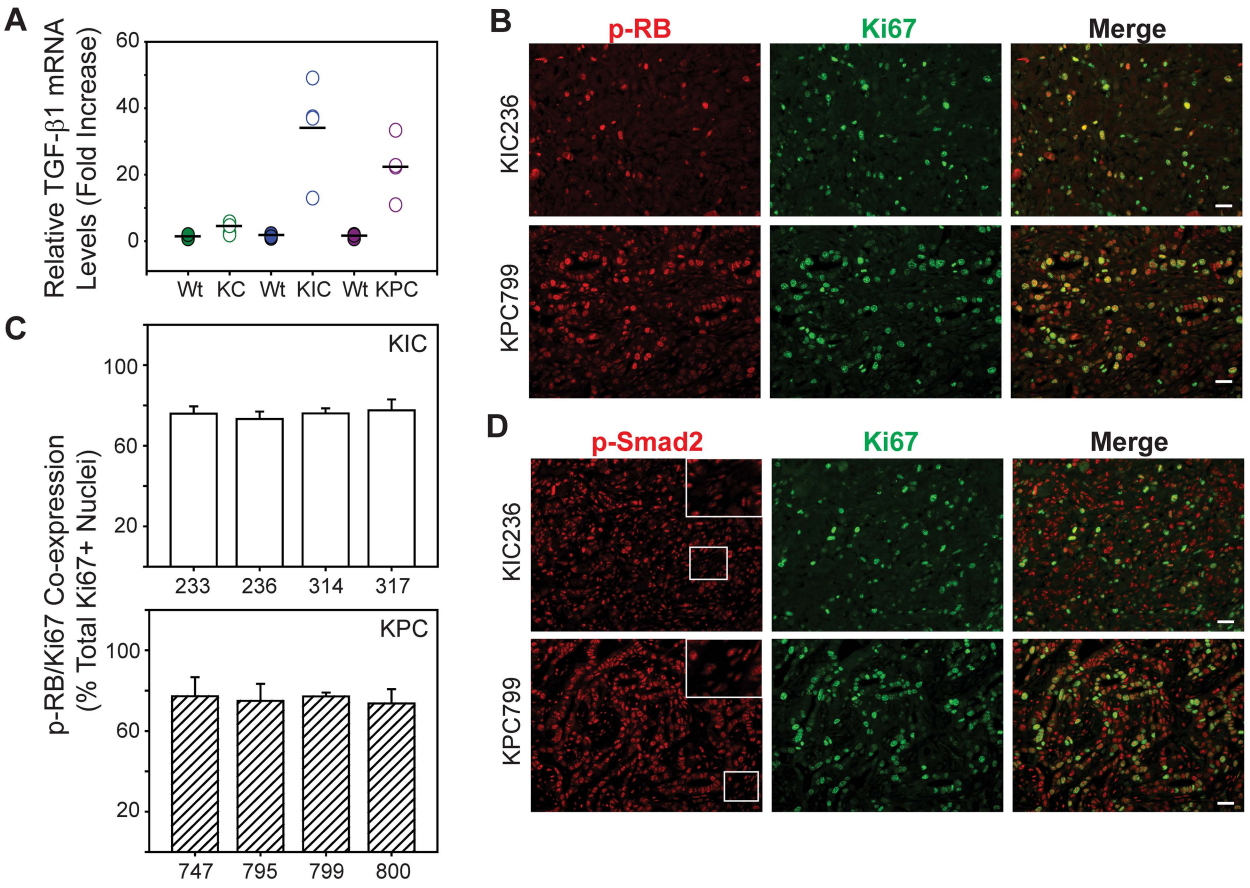

Supplemental Figure 3. TGF-β1 is elevated in KIC and KPC pancreata that harbor proliferating PCCs with inactive RB and active Smad2. **(A)** Compared to KC pancreata (open green circles), TGF-β1 mRNA levels are elevated in KIC (open blue circles) and KPC (open purple circles) pancreata. Closed circles represent wild-type (Wt) littermate controls for KC (green), KIC (blue) and KPC (purple) mice. Horizontal bars denote mean expression levels in four different mice. **(B)** p-RB (red) is abundant in KIC and KPC mPDAC and frequently overlaps with Ki67-positive (green) cells as evidenced by the overlay (merge). **(C)** Quantitation shows that p-RB is detected in 76% of Ki67-positive PCCs in four different KIC and KPC pancreata. Data are presented as mean % ± SEM. **(D)** p-Smad2 (red) is abundant in KIC and KPC mPDAC and adjacent stromal cells (insets; magnified images of boxed areas), and is detected in all Ki67-postivive PCCs (green,) as evidenced by the overlay (merge). (A) and (C) are representative images from one of four different two month old KIC (KIC236) and KPC (KPC799) pancreata. Scale Bars, 50 μm.

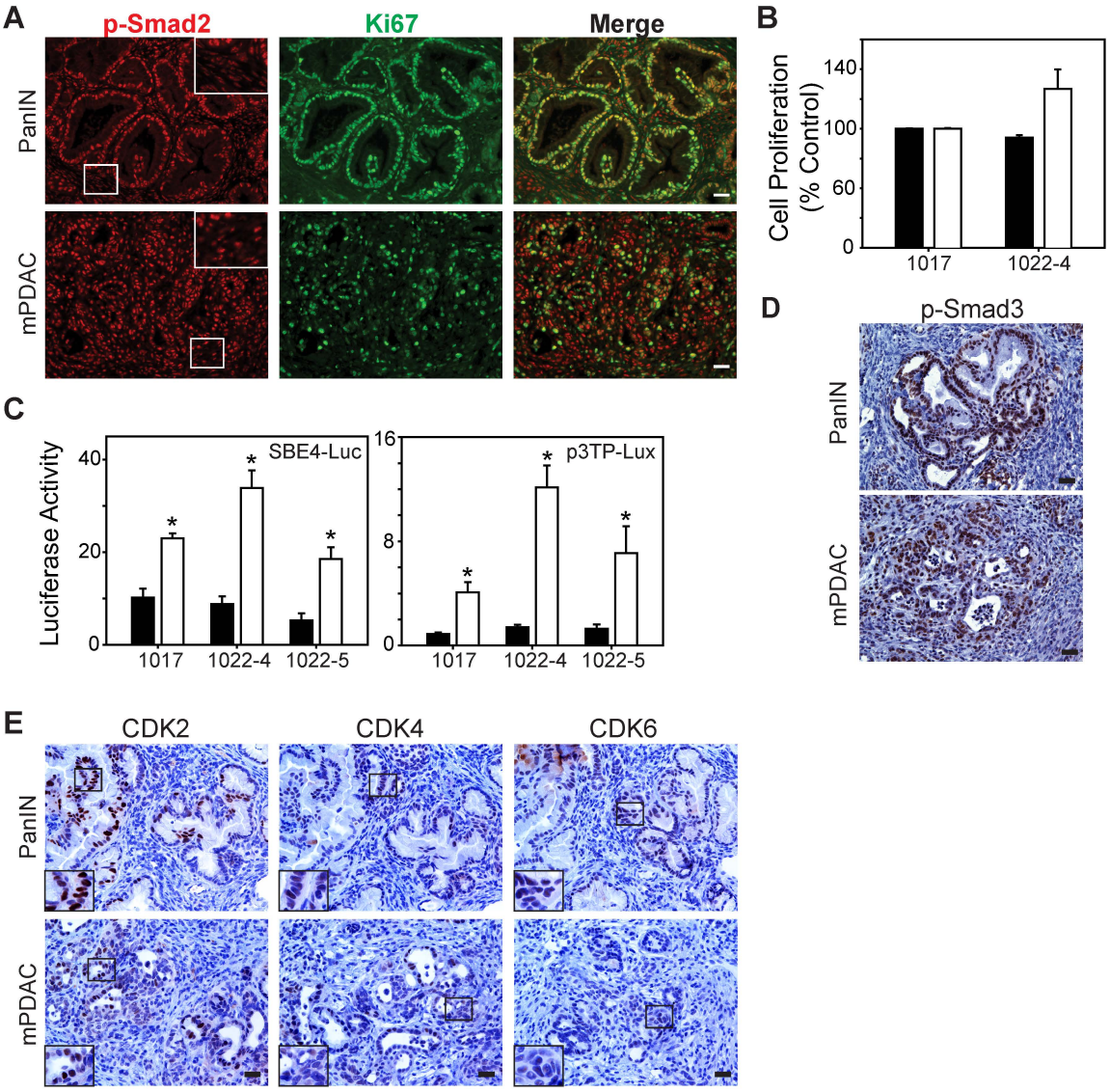

Supplemental Figure 4. Smad-dependent pathways are active in KRC PCCs that are resistant to TGF-β1-mediated growth inhibition. **(A)** p-Smad2 (red) is abundant in KRC PanIN, mPDAC and adjacent stromal cells (insets; magnified images of the boxed areas), and is detected in all Ki67-positive cells (green) as evidenced by the overlay (merge). **(B)** Sham-transduced KRC1017 cells are resistant to TGF-β1 (open bars, [0.5 nM]) growth inhibition, whereas sham-transduced KRC1022-4 cells are growth-stimulated. **(C)** Luciferase assays show that compared to control-treated cells (black bars), TGF-β1 (open bars) signficantly enhances the activity of SBE4-Luc and p3TP-Lux in KRC cells. SBE4-Luc: $P<.018$. p3TP-Lux: $P<.036$. **(D)** Phospho-Smad3 (p-Smad3) is abundant in the nuclei of KRC PanIN and mPDAC. **(E)** KRC PanIN and mPDAC exhibit stong nuclear CDK2 immunoreactivity, whereas CDK4 and CDK6 immunoreactivity is weak and less abundant. Shown in (A), (D) and (E) are representative images from one of four different two month old KRC pancreata. Scale Bars, 50 μm.

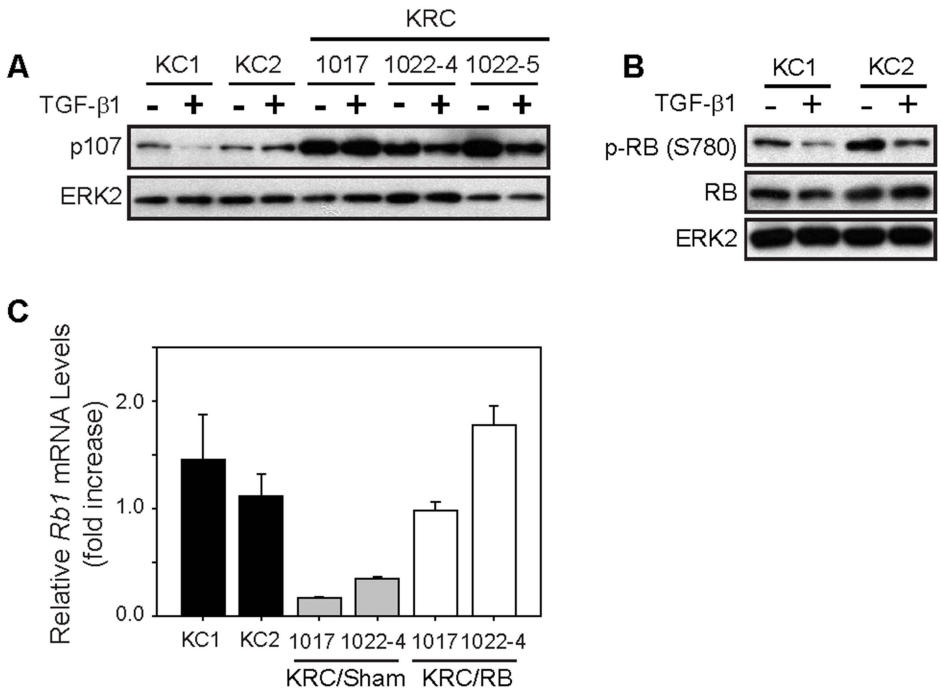

Supplemental Figure 5. p107 is up-regulated in KRC cells and TGF-β1 hypophosphorylates RB in KC cells. **(A)** p107 is up-regulated in KRC cells by comparison with KC cells, and is down-regulated by TGF-β1 [0.5 nM] in KC1 and KRC1022-5 cells. **(B)** TGF-β1 [0.5 nM] markedly attenuates phospho-RB (p-RB(S780)), but not total RB (RB) in KC cells. Shown in (A-B) are representative blots from three independent experiments. ERK2 confirms equivalent lane loading. **(C)** qPCR shows that compared to Sham (gray bars), RB restoration in KRC cells (open bars) increases *Rb1* mRNA to the same levels as KC cells (closed bars). Data are presented as the mean ± SEM from three independent experiments.

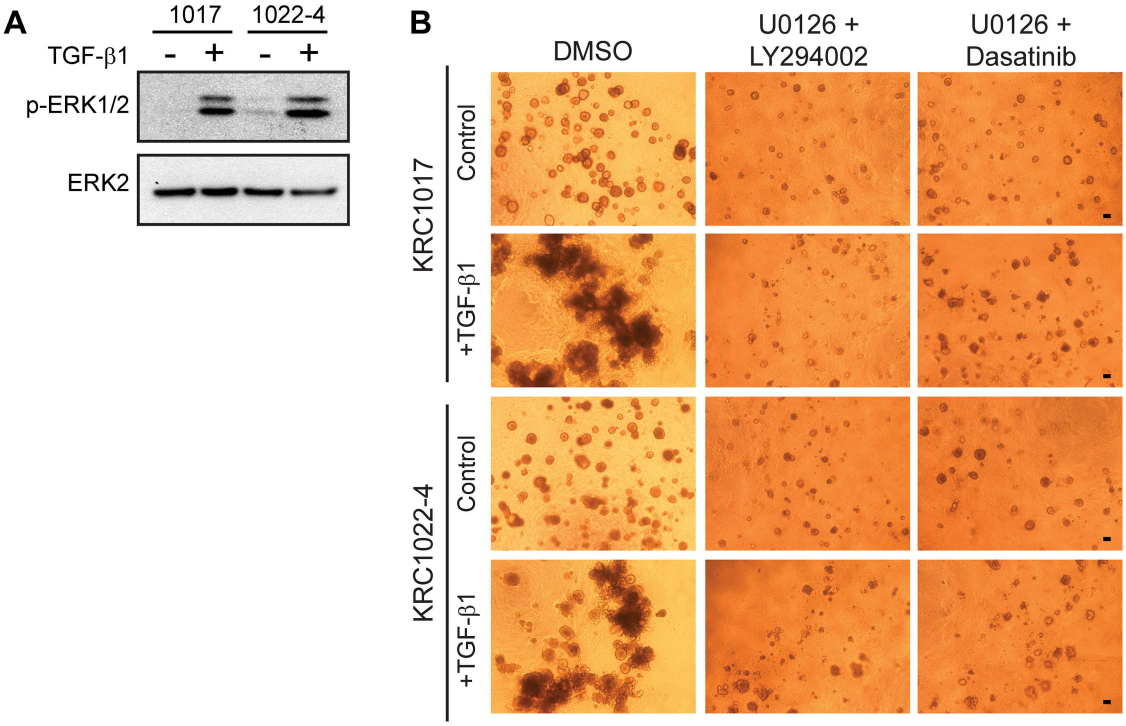

Supplemental Figure 6. TGF-β1 enhances ERK phosphorylation and combined MAPK and PI3K or Src inhibtion blocks TGF-β1-enhanced KRC growth. **(A)** TGF-β1 ([0.5 nM], 15 min) markedly increases phosphorylation of ERK1 and ERK2 (p-ERK1/2) in KRC1017 and KRC1022-4 cells. Shown is a representative blot from three independent experiments. ERK2 confirms equivalent lane loading. **(B)** In the absence of inhibitors (DMSO, left panels), TGF-β1 (second and fourth rows) stimulates KRC growth, but in the presence of MAPK and PI3K (U0126+LY294002, middle panels) or MAPK and Src (U0126+dasatinib, right panels) inhibitors, growth stimulation is markedly attenuated. Shown are representative images from three independent experiments on day 14. Scale Bars, 50 μm.

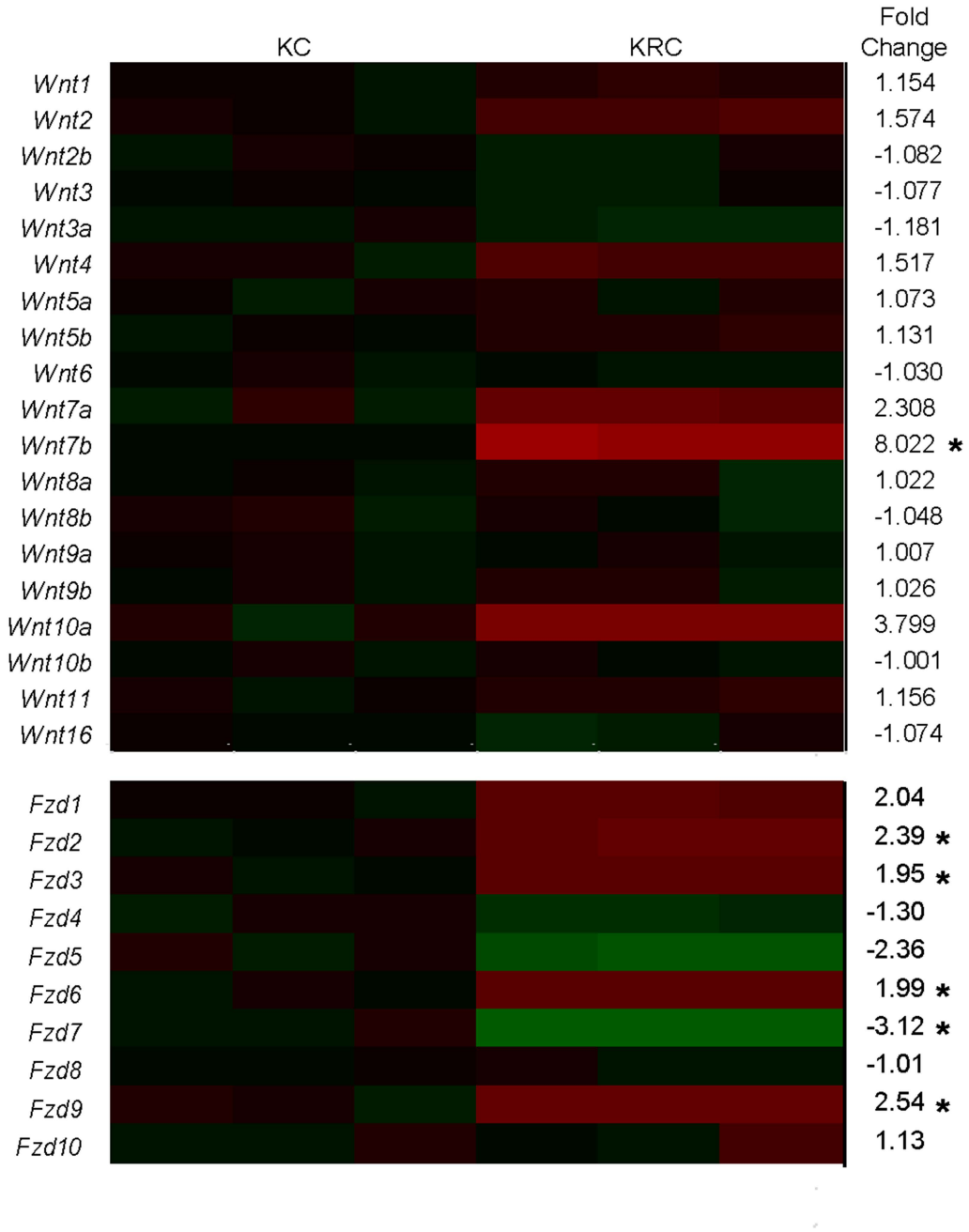

Supplemental Figure 7. Wnt7b and Wnt receptor mRNAs are up-regulated in KRC cells.
A heatmap of all Wnt ligands and their receptors derived from triplicate microrrays using RNA isolated from KC and KRC cells shows that *Wnt7b* and *Fzd2*, *3*, *6* and *9* are up-regulated in KRC cells, by comparison with KC cells, whereas *Fzd7* is significantly down-regulated.

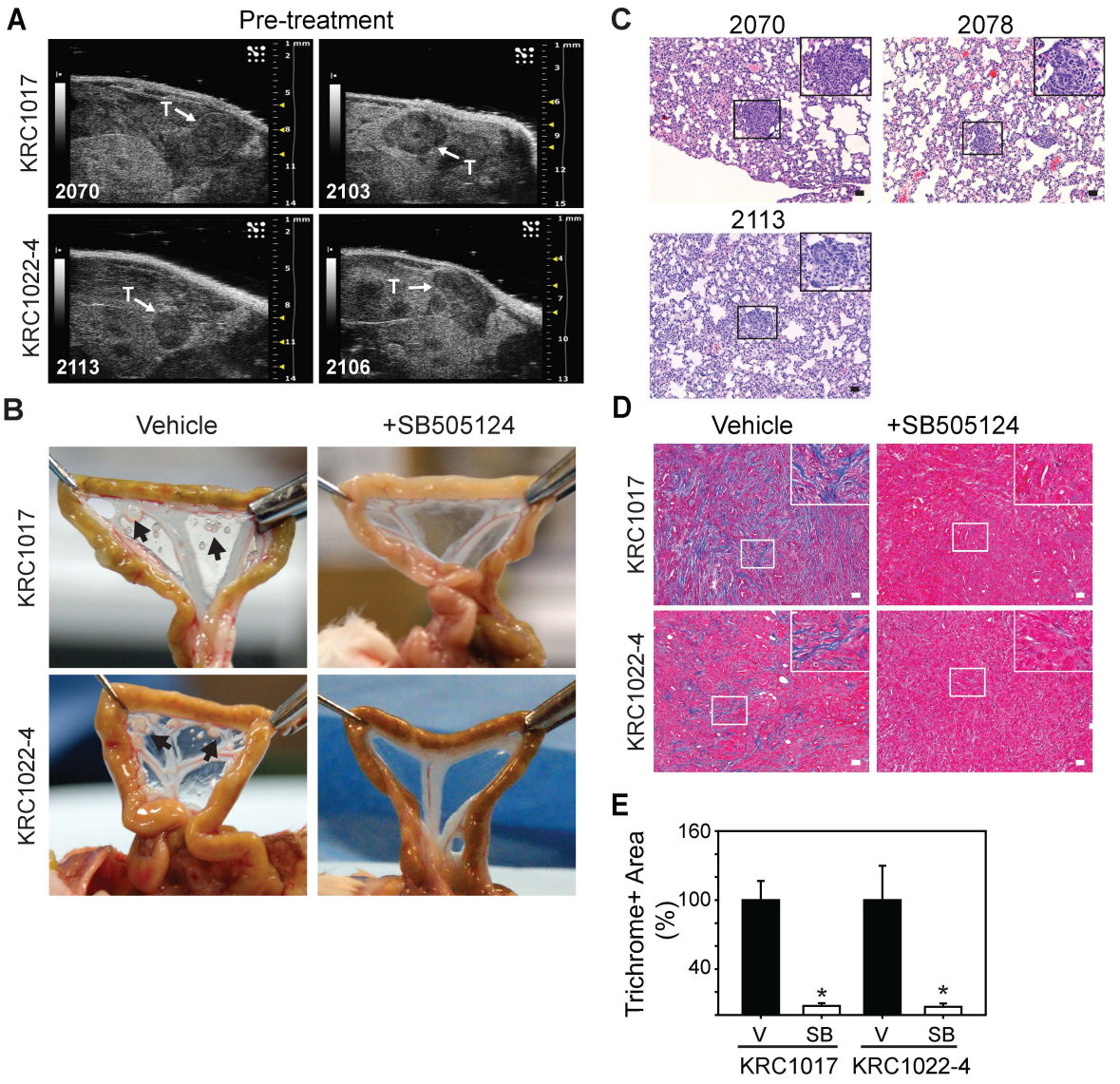

Supplemental Figure 8. SB505124 attenuates metastasis and stroma formation in a syngeneic orthotopic model. **(A)** High resolution ultrasound images show that before treatment, mice had similar size tumors (T, arrows). Shown are representative images from 4 mice. **(B)** Peritoneal seeding, evidenced by mesenteric metastases, is abundant in vehicle-treated mice (arrows), but absent in SB505124-treated mice. Shown are images at necropsy on days 19 (Vehicle), or 47 (SB505124). **(C)** H&E staining shows that three vehicle-treated mice have lung metastases. Insets show magnified images of metastatic lesions (boxed). **(D)** Masson's trichrome staining shows that SB505124 markedly reduces stroma within the tumor mass. Shown are representative images from 1 mouse per treatment group, and insets show magnified images of boxed areas. In (C)-(D), Scale Bars, 50 μm. **(E)** Quantitation shows that compared to vehicle (V, closed bars), SB505124 (SB, open bars) significantly reduces trichrome-positive staining. *, $P<.03$. Data are presented as mean % ± SEM.

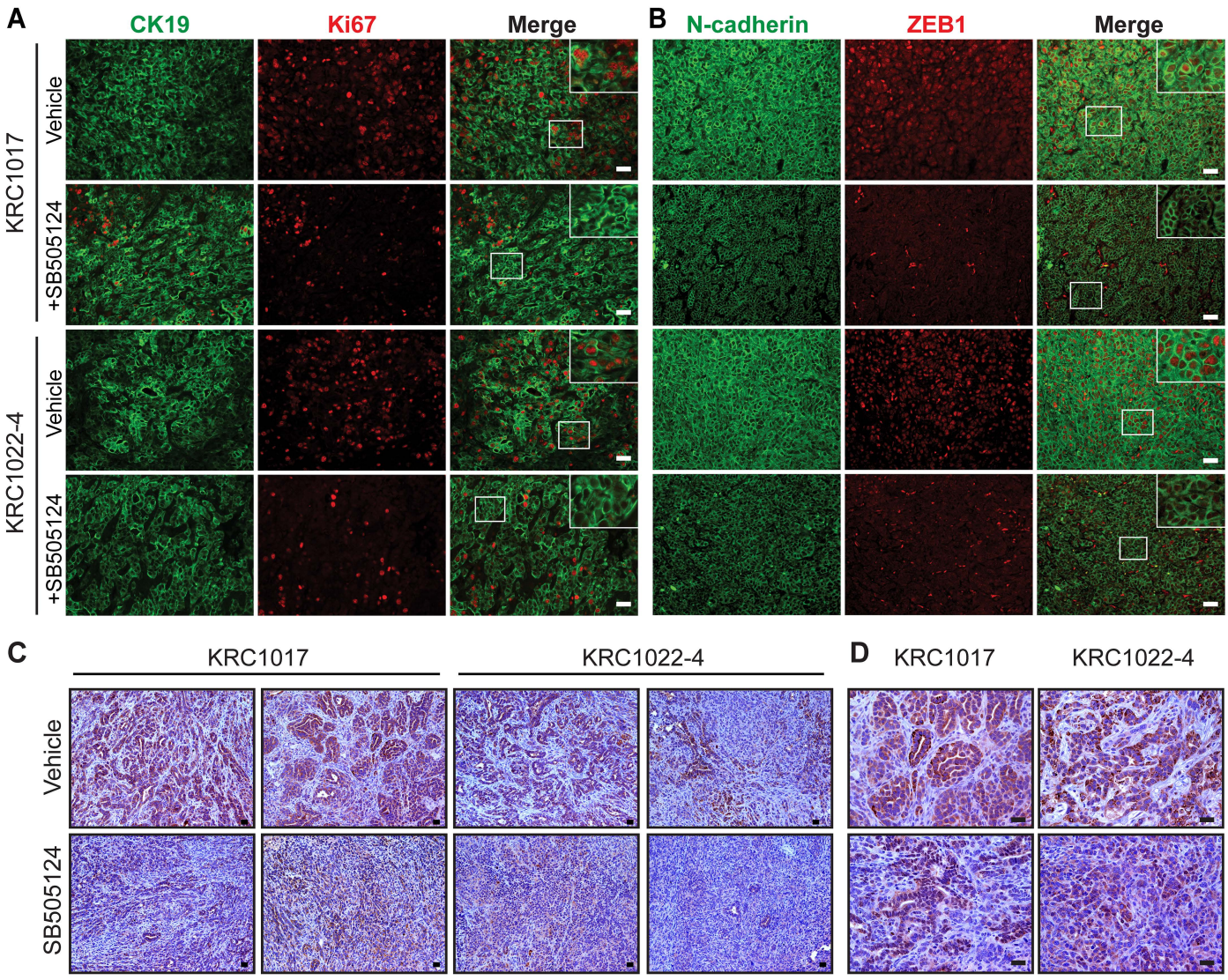

Supplemental Figure 9. SB505124 attenuates PCC proliferation, and mesenchymal marker and Wnt7b expression in a syngeneic orthotopic model. **(A)** In vehicle-treated mice, CK19-positive PCCs (green) frequently co-express nuclear Ki67 (red) as evidenced by the overlay (merge; insets show magnified images of boxed areas), whereas in SB505124-treated mice Ki67 immunoreactivity in CK19-positive PCCs is markedly reduced. **(B)** PCCs in vehicle-treated mice display strong N-cadherin immunoreactivity (green) and abundant nuclear Zeb1 (red) as evidenced by the overlay (merge; insets show magnified images of boxed areas), whereas PCCs in SB505124-treated mice have reduced N-cadherin expression, evidenced by decreased fluorescence intensity, and rare Zeb1-positive nuclei. **(C)** PCCs in SB505124-treated mice have attenuated Wnt7b immunoreactivity by comparison to PCCs in vehicle controls. **(D)** Some foci of PCCs in SB505124-treated mice exhibit moderate to strong Wnt7b immunoreacitvity, but the intensity of the signal is lower than in corresponding foci in vehicle-treated mice. Shown in (A-B) and (D) are representative images from 1 mouse per treatment group, in (C) 2 mice. Scale Bars, 50 μm.

Wnt7b-Luc Fwd	5’ CCATTTGATGCTGCTGTCCGG
Wnt 7b-Luc Rev	5’ CTCACCATGGTGGCAACGCGTGC

Wnt 7b-ΔSBE1-Fwd	5’ Phos/CTAGCTGTGACAGGCAGTGTC
Wnt7b-ΔSBE1-Rev	5’ Phos/ACGCTATGTAGCACAGCGGACCAGCTAGTAA

Wnt7b-ΔSBE2-Fwd	5’ Phos/CATAGCGTACACCCGCCCGCATCGGACA
Wnt7b-ΔSBE2-Rev	5’ Phos/ATTCTTGTTGAACCGCTAAAGTGG

ChIP-Fwd	5’ CCATTTGATGCTGCTGTCCGG
ChIP-Rev	5’ AGGTAACAATGCCTGATCCGG

Supplemental Table 1. Primer sequences for construction of Wnt7b luciferase (Wnt7b-Luc), mutation of both SBEs in Wnt7b-Luc (Wnt7b-DSBE-Luc) and for Wnt7b ChIP assays.